



HAL
open science

Determination of the semiexperimental equilibrium structure of 2-acetylthiophene in the presence of methyl internal rotation and substituent effects compared to thiophene

Christina Dindić, Jil Ludovicy, Vladimir Terzi, Arne Lüchow, Natalja Vogt,
Jean Demaison, Ha Vinh Lam Nguyen

► To cite this version:

Christina Dindić, Jil Ludovicy, Vladimir Terzi, Arne Lüchow, Natalja Vogt, et al.. Determination of the semiexperimental equilibrium structure of 2-acetylthiophene in the presence of methyl internal rotation and substituent effects compared to thiophene. *Physical Chemistry Chemical Physics*, 2022, 24, pp.3804-3815. 10.1039/D1CP04478H . hal-03592004

HAL Id: hal-03592004

<https://hal.science/hal-03592004>

Submitted on 1 Mar 2022

HAL is a multi-disciplinary open access archive for the deposit and dissemination of scientific research documents, whether they are published or not. The documents may come from teaching and research institutions in France or abroad, or from public or private research centers.

L'archive ouverte pluridisciplinaire **HAL**, est destinée au dépôt et à la diffusion de documents scientifiques de niveau recherche, publiés ou non, émanant des établissements d'enseignement et de recherche français ou étrangers, des laboratoires publics ou privés.

Determination of the semiexperimental equilibrium structure of 2-acetylthiophene in the presence of methyl internal rotation and substituent effects compared to thiophene

Christina Dindić^a, Jil Ludovicy^a, Vladimir Terzi^a, Arne Lüchow^a, Natalja Vogt^{b,c}, Jean Demaison^b, Ha Vinh Lam Nguyen^{d,e*}

^a Institute of Physical Chemistry, RWTH Aachen University, Landoltweg 2, 52074 Aachen, Germany

^b Section of Chemical Information Systems, University of Ulm, Albert-Einstein-Allee 47, 89081 Ulm, Germany

^c Department of Inorganic Chemistry, Lomonosov Moscow State University, 119991 Moscow, Russian Federation

^d Univ Paris Est Creteil and Université de Paris, CNRS, LISA, 94010 Créteil, France

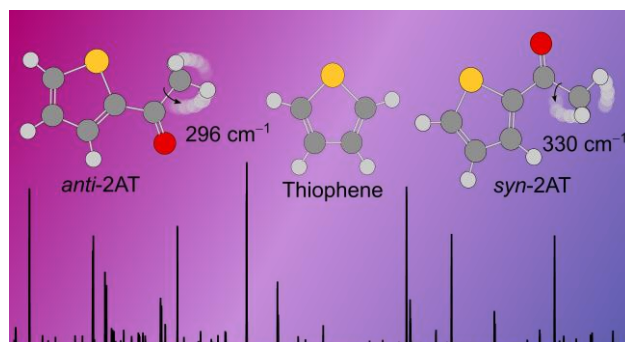
^e Institut Universitaire de France (IUF), 75231 Paris cedex 05, France

* Corresponding author. Email: lam.nguyen@lisa.ipsl.fr

Abstract

The microwave spectra of thiophene and 2-acetylthiophene were recorded in the frequency range from 2 to 40 GHz using two molecular jet Fourier transform microwave spectrometers. For 2-acetylthiophene, two conformers with a *syn* and an *anti* orientation of the S1–C2 and C6=O bonds (with respect to the C2–C6 bond) were identified, where the *syn*-conformer is more stable. The spectra of the ³⁴S- and ¹³C-isotopologues of *syn*-2-acetylthiophene were also assigned, and the semiexperimental equilibrium structure could be determined. Compared to thiophene, at the substitution position, the S1–C2 and C2=C3 bond lengths both increase by about 0.007 Å, and the bond angle S1–C2=C3 decreases by 0.06°, noticeably larger than the experimental uncertainties. A-E torsional splittings were observed due to internal rotation of the methyl group hindered by a barrier height of 330.187(35) and 295.957(17) cm⁻¹ for the *syn*-conformer and the *anti*-conformer, respectively. Geometry and internal rotation parameters are compared with those of related thiophene derivatives, as well as those of furan and 2-acetylthiophene to gain a better understanding of structure determination in the presence of methyl internal rotation.

Graphical abstract



1. Introduction

Over the history of microwave spectroscopy, methyl internal rotation has always been a subject of special interest alongside structural chemistry as the classic topic [1,2]. When the molecule contains a methyl rotor with a finite torsional barrier, torsional fine structures of all rotational transitions in form of A-E doublets are observed [3]. If the methyl group is attached to a system containing conjugated π -double bonds, the behavior of the methyl internal rotation becomes unpredictable, because the delocalization of π -electrons can transfer electronic effects through the entire π -system. Acetyl methyl rotors are known to be sensitive to the structure of the moiety attached at the other side of the carbonyl bond, expressed through the torsional barrier. For example, the C_1 conformers of methyl *n*-alkyl ketones exhibit barriers to methyl internal rotation of about 240 cm^{-1} , while values found for the C_s conformers are approximately 180 cm^{-1} [4-7]. The torsional barrier increases significantly to about 600 cm^{-1} in acetophenone derivatives where a phenyl ring is attached to the carbonyl group [8] or to 430 cm^{-1} for the *antiperiplanar* conformers and 350 cm^{-1} for the *synperiplanar* conformers of α,β -unsaturated ketones [9]. Recently, we investigated 2-acetylfuran where we observed a barrier height of 319 cm^{-1} for the *anti*-conformer and 240 cm^{-1} for the *syn*-conformer [10]; both values do not fit in any of the categories classified by Andresen et al. [7,9]. This suggests that if an aromatic heterocycle is involved in conjugation with the carbonyl group, special classes might be required. Therefore, we are interested in 2-acetylthiophene (2AT, illustrated in Figure 1), the sulphur analogue of 2-acetylfuran, on the one hand to compare the torsional barriers. It is known in the literature that the barriers to methyl internal rotation in oxygen analogues are higher than those in sulphur analogues. Some examples of the barriers in general cases are dimethyl sulphide (735.8 cm^{-1}) [11] vs dimethyl ether (944.3 cm^{-1}) [12] or methyl thioformate (127.5 cm^{-1}) [13] vs methyl formate (370.9 cm^{-1}) [14]. For molecules containing a furan or thiophene moiety, available examples are 194.1 cm^{-1} for 2-methylthiophene [15] vs. 416.2 cm^{-1} for 2-methylfuran [16], 258.8 cm^{-1} for 3-methylthiophene [17] vs. 380.5 cm^{-1} for 3-methylfuran [18], or 248.0 cm^{-1} for 2,5-dimethylthiophene [19] vs. 439.1 cm^{-1} for 2,5-dimethylfuran [20]. Surprisingly, this is no longer true if the methyl group is separated from the ring by a carbonyl group, as will be explored in this work. On the other hand, 2AT will yield a data point as the prototype molecule towards establishing a possible “thiophene class” to predict methyl torsional barriers for acetyl group containing ketones [7,9].

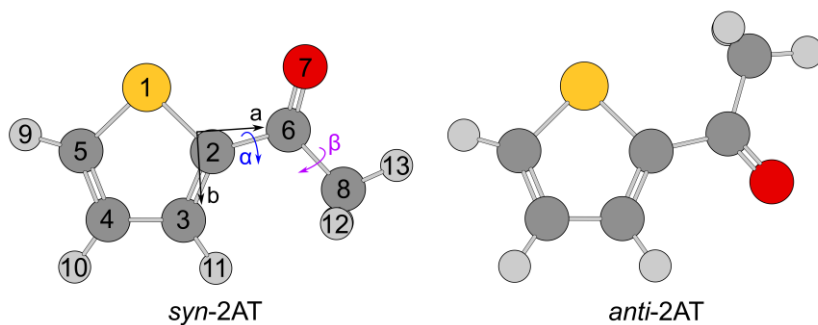


Figure 1: The two conformers of 2AT, *syn* and *anti*. Atom numbering, dihedral angles and principal axis are marked at *syn*-2AT. H14 lies behind H12. The sulphur atom is marked in yellow, oxygen in red, carbon atoms are in dark grey and hydrogen atoms in light grey.

Another aspect of this work focuses on the classic topic of microwave spectroscopy on structure determination. While for a rigid rotor molecule a Hamiltonian model consisting of a rigid rotor part supplemented by centrifugal distortion terms is sufficient to model the spectrum to measurement accuracy, this is no longer the case if a methyl internal rotor is present in the molecule. Additional terms taking into account the A-E splittings mentioned previously strongly perturb the structural parameters, notably the three rotational constants used for structure determination purposes. Though it is known that substitution on an aromatic ring changes the structural parameters such as bond lengths and bond angles at the substituted position [21-25], obtaining this information in the case of 2AT is challenging as highly precise structural parameters are required, which in turn needs an appropriate Hamiltonian model to treat the methyl internal rotation.

In the present work, we combine microwave spectroscopy with quantum chemical calculations at moderate levels to assign two conformers of 2AT, *anti* and *syn*, to deduce with high accuracy the rotational constants using the program *XIAM* employing the combined axis method to treat the methyl internal rotation, as well as to determine the torsional barrier for both conformers. For the more stable *syn*-conformer, we observed spectra of the ^{34}S and all ^{13}C isotopologues and could determine its semiexperimental equilibrium structure r_e^{SE} . For the *anti*-conformer, only spectra of the ^{34}S and two ^{13}C isotopologues were detectable. The r_e^{SE} structure is compared with accurate *ab initio* structures. To study structural changes induced by substitution, we measured the spectrum of thiophene and its ^{34}S and ^{13}C isotopologues in the frequency range from 2 to 40 GHz and compared the r_e^{SE} structure of thiophene with that of 2AT, paying special attention to the S1–C2 and C2=C3 bond lengths, as well as the S1–C2=C3 bond angle.

2. Quantum chemical calculations

2.1. Conformational analysis of 2AT

As the thiophene ring is known to be planar [26,27] and the rotation of the methyl group does not create new conformers, the only structural element determining the conformations of 2AT is the acetyl group. For the conformational analysis, the dihedral angle $\alpha = \angle(\text{S1}-\text{C2}-\text{C6}=\text{O7})$ (for atom numbering see Figure 1) was varied in steps of 10° and all other geometry parameters were optimized with the MP2 [28] and B3LYP [29,30] methods in combination with Pople's basis set 6-311++G(d,p) [31] using the *Gaussian 16* program package [32]. The D3 model of Grimme [33] with Becke-Johnson (BJ) damping [34] was added to take into account the dispersion interactions. These two different methods were employed, since many previous investigations have reported method-dependent discrepancies between optimized structures [35,36]. The potential energy curves drawn in Figure 2 using coefficients from a Fourier expansion given in Table S-1 of the Electronic Supporting Information (ESI) show that it is also the case for 2AT. Both the MP2 and B3LYP methods agree on one distinct minimum at $\alpha = 0^\circ$, corresponding to a *syn* orientation of the oxygen and the sulphur atoms of 2AT, but at $\alpha = 180^\circ$ the B3LYP-D3BJ curve possesses one minimum corresponding to a planar *anti*-conformation, contrasting with the double minimum obtained for the MP2 curve.

2.2. Geometry optimizations

Subsequently, optimizations of the structures with the *synperiplanar* and *antiperiplanar* S1–C2–C6=O fragments under full geometry relaxation including frequency calculations yielded the fully optimized structures (called *syn* and *anti*, respectively, see Figure 1) as well as confirmed them to be stable. Their nuclear coordinates optimized at the B3LYP-D3BJ level of theory are given in Table S-2 in the ESI. The calculated rotational constants, dipole moments, dihedral angles and energy differences obtained at both levels are listed in Table 1. Benchmark structure optimizations were also carried out using various basis sets in combination with the MP2, B3LYP-D3, B3LYP-D3BJ, M06-2X [37], ω B97X-D [38] and coupled cluster theory including single and double excitation (CCSD) [39] methods. The rotational constants derived from all optimized structures are listed in Table S-3 in the ESI and will be discussed later in relation to the experimentally determined values. At all levels of theory, the *syn*-conformer is energetically more favourable with an energy difference from about 2.1 to 6.2 $\text{kJ}\cdot\text{mol}^{-1}$ (see Table S-3). Therefore, it was questionable whether both conformers could be observed in the microwave spectrum under our molecular jet conditions where the rotational temperature is only about 1 – 2 K.

Table 1: Calculated rotational constants, dipole moments, dihedral angles and relative energies for the two conformers of 2AT. For both MP2 and B3LYP-D3BJ methods, the 6-311++G(d,p) basis set was used.

Par.	Unit	MP2		B3LYP-D3BJ	
		<i>syn</i>	<i>anti</i>	<i>syn</i>	<i>anti</i>
A_e	MHz	3554.5554	3528.4064	3558.9758	3526.8413
B_e	MHz	1414.4817	1414.7173	1409.8986	1412.6037
C_e	MHz	1018.2769	1019.3106	1016.2252	1014.9726
μ_a	D	-2.03	2.75	-1.97	-2.59
μ_b	D	3.84	-1.95	3.30	-1.80
μ_c	D	0.00	-0.38	0.00	0.00
α	°	0.00	173.97	-0.02	180.00
ΔE^a	kJ/mol	0	5.73	0	2.58

^a Energy including zero-point corrections relative to that of the more stable conformer *syn*-2AT with $E_{MP2} = -704.231465$ Hartree and $E_{B3LYP-D3BJ} = -705.7934819$ Hartree.

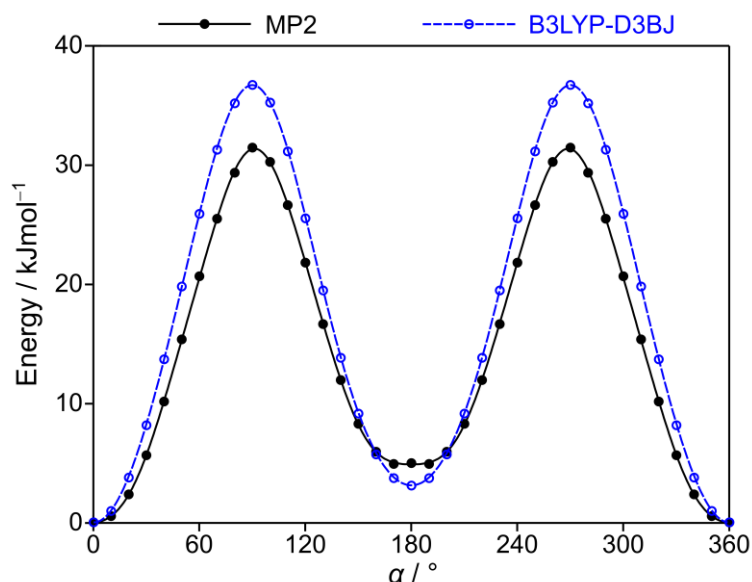


Figure 2: The potential energy curves of 2AT obtained by rotating the acetyl group about the C2–C6 bond (for atom numbering see Figure 1) by varying the dihedral angle α in a grid of 10°. Calculations were performed at the MP2/6-311++G(d,p) and B3LYP-D3BJ/6-311++G(d,p) levels of theory. The relative energies are given in respect to the lowest energy conformation with $E_{MP2} = -704.3348246$ Hartree and $E_{B3LYP-D3BJ} = -705.7934819$ Hartree.

To calculate the r_e^{B0} structure of thiophene and both conformers of 2AT, geometry optimizations were performed using two *ab initio* levels of theory, MP2 and CCSD, where the latter is augmented with a perturbational estimate of the effects of connected triple excitations, CCSD(T) [40]. The cc-pwCVnZ basis sets with $n = T, Q$ were employed with all electrons being correlated (ae) [41]. For the calculation of the anharmonic force field the double hybrid functional B2PLYP-D3 [42] was employed with the split-valence Pople 6-311+G(3df,2pd) basis functions. The CCSD(T) as well as some MP2 calculations were performed with the Molpro program [43,44], while for the B2PLYP calculations, the *Gaussian 16* program package [32] was used.

2.3. Methyl internal rotation

The barrier to internal rotation for the acetyl methyl group of 2AT was predicted by varying the dihedral angle $\beta = \angle(\text{C2-C6-C8-H12})$ in 10° steps between 0° and 360° . The resulting potential energy curves for both conformers calculated at the MP2 and B3LYP-D3BJ/6-311++G(d,p) levels of theory are shown in Figure 3. For the *syn*-conformer the potential exhibits the typical threefold symmetry expected for a methyl group. The predicted torsional barrier is 320.5 cm^{-1} (MP2) or 220.8 cm^{-1} (B3LYP). The corresponding values for the *anti*-conformer are 284.6 cm^{-1} and 193.6 cm^{-1} . For *anti*-2AT, the MP2 potential exhibits a double minimum around 60° , 180° and 300° due to a switch between the two non-planar structures, whereas B3LYP-D3BJ predicts a threefold potential. The Fourier coefficients of the parameterised potentials are given in Table S-4 in the ESI.

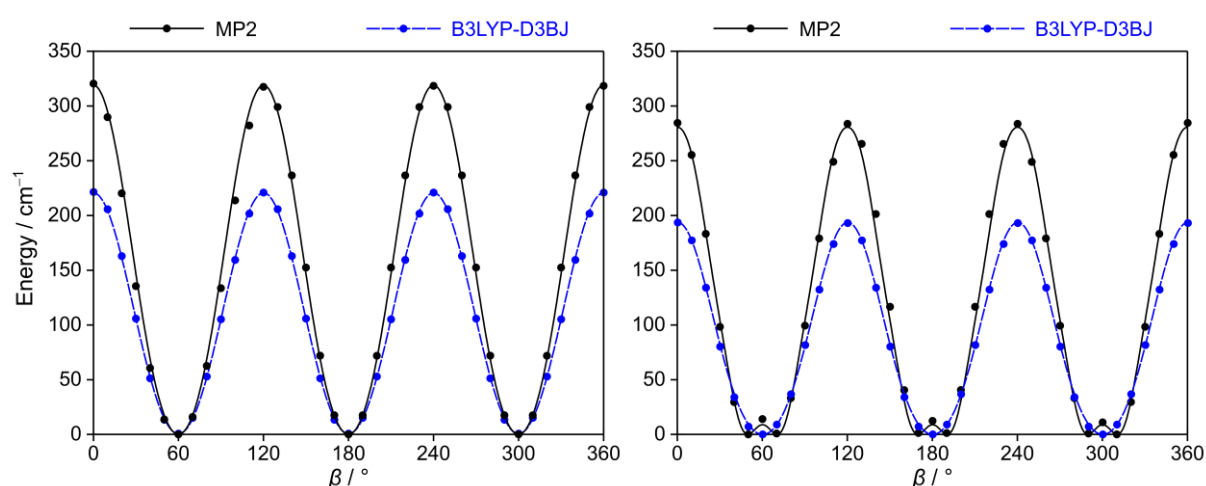


Figure 3: Potential energy curves of *syn*-2AT (left hand side) and *anti*-2AT (right hand side) obtained by rotating the acetyl methyl group about the C6–C8 bond in 10° steps. The MP2 and B3LYP-D3BJ/6-311++G(d,p) levels of theory were used. The predicted torsional barriers are

320.5 cm^{-1} and 220.8 cm^{-1} for *syn*-2AT, as well as 284.6 cm^{-1} and 193.6 cm^{-1} for *anti*-2AT, respectively.

3. Microwave Spectroscopy

3.1. Measurements

The microwave spectra were recorded using two molecular jet FTMW spectrometers operating in the frequency range from 2 to 40 GHz [45,46]. The substances were purchased from Sigma-Aldrich, Schnelldorf, Germany, with a stated purity of 98 % and used without any further purification. For 2AT, a scan from 9.0 to 15.4 GHz was recorded as a series of overlapping spectra with a step width of 0.25 MHz, which is the resolution of the scan frequencies. The substance was placed on a 5 cm piece of pipe cleaner and inserted upstream of the nozzle. Helium with a backing pressure of about 2 bar was flown over the sample and carried the substance into the cavity. A portion of the scan is illustrated in Figure 4. Each line of the scan was initially measured with 50 co-added free-induction decays and then subsequently remeasured at a higher resolution with an experimental accuracy of 2 kHz [47]. After the spectrum was assigned, measurements outside of the survey spectrum were carried out. For thiophene, a gas mixture containing about 2% substance in helium at a total pressure of 1.2 bar was used. Only high resolution measurements were needed for thiophene because the rotational constants are known from the literature [27,48].

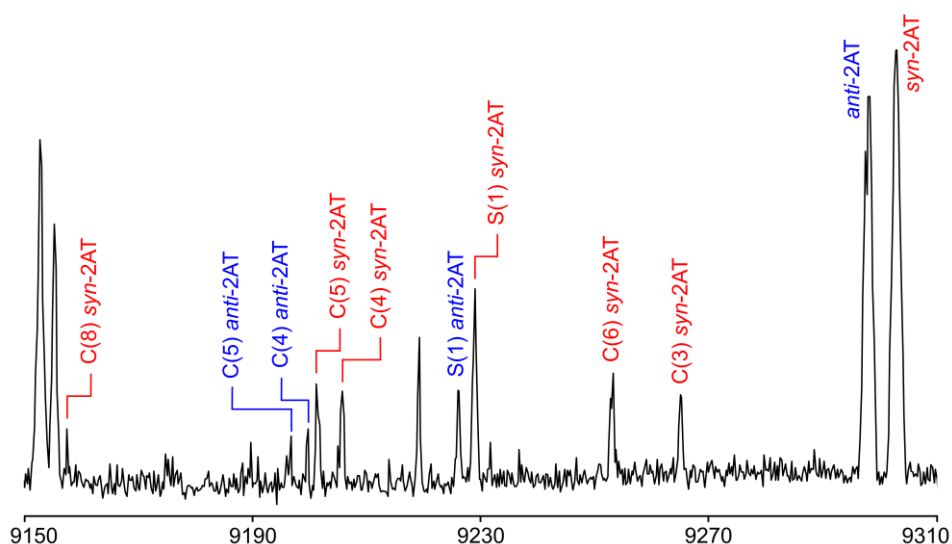


Figure 4: A portion of the scan of 2AT in the frequency range from 9150 to 9310 MHz recorded by overlapping spectra with 50 co-added decays per each spectrum. Lines belonging to the $4_{04} \leftarrow 3_{03}$ transition are labelled with the corresponding conformer, ^{34}S - or ^{13}C -isotopologue, as well as the atom position in parentheses. The intensities are given in a logarithmic scale in an arbitrary unit. The temperature of the molecular jet was approximately 1-2 K.

3.2. 2-Acetylthiophene

3.2.1. Spectrum assignment

The assignment was started using the rotational constants calculated at the MP2/6-311++G(d,p) level of theory listed in Table 1. As the *syn*-conformer was predicted to be energetically more favourable, a rigid rotor spectrum was predicted first for this conformer and compared with the survey spectrum. From values of the calculated dipole moments (see Table 1), only *a*- and *b*-type transitions were expected.

The rigid rotor assignment was straightforward with the measurement accuracy of the scan (250 kHz) as the predicted rotational constants were adequately close to the experimental ones. However, when the high resolution measurements were analysed, the assignment became more difficult. The transition $3_{03} \leftarrow 2_{02}$ shown in Figure 5 exemplifies that the line frequencies of the *syn*- and *anti*-conformers are often very close to each other due to their similar rotational constants (see Table 1). Furthermore, splittings arising from the internal rotation of the methyl group are also in the same order of magnitude, making the correct assignment of the conformational and torsional species even more challenging. Nevertheless, transitions of both conformers including their torsional splittings could be eventually assigned. The resulting global fits and molecular parameters obtained with the *XIAM* program [49] are summarised in Table 2; the assigned frequencies are listed in Tables S-5 and S-6 in the ESI. In total 138 A- and 174 E-species transitions were assigned for *syn*-2AT, as well as 117 and 128 transitions, respectively, for *anti*-2AT.

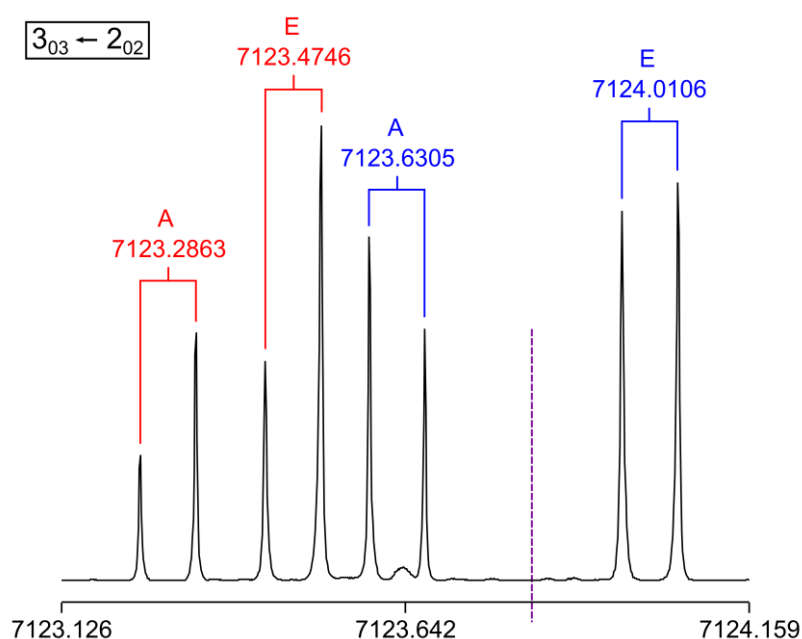


Figure 5: A high resolution measurement of the $3_{03} \leftarrow 2_{02}$ transition of 2AT recorded at 7123.83 MHz (shown as a dotted line). For this spectrum 153 decays were co-added. The splittings

indicated by brackets are caused by the Doppler effect; the mean frequency is the transition frequency. The A-E torsional splitting is 188.3 kHz and 380.1 kHz for *syn*-2AT (red) and *anti*-2AT (blue), respectively.

Table 2: Experimental spectroscopic parameters of the *anti*- and *syn*-conformers of 2AT obtained with the program *XIAM*.

Par. ^a	Unit	<i>syn</i>	<i>anti</i>
A_0	MHz	3588.05339(29)	3555.438(21)
B_0	MHz	1415.91822(11)	1418.7605(47)
C_0	MHz	1022.074502(72)	1020.7702(47)
D_J	kHz	0.05417(64)	0.05274(35)
D_{JK}	kHz	0.0470(51)	0.0755(39)
D_K	kHz	0.3743(89)	0.359(17)
d_1	kHz	-0.01724(41)	-0.01719(21)
d_2	kHz	-0.00223(25)	-0.002105(98)
V_3	cm ⁻¹	330.187(35)	295.957(17)
$D_{p_i^2 J}$	kHz		41.06(48)
$D_{p_i^2 K}$	MHz	-0.1311(53)	-0.1239(19)
$\angle(i, a)$	deg	47.937(23)	61.6587(72)
$\angle(i, b)$	deg	42.063(23)	28.3413(72)
$\angle(i, c)$	deg	90.0 ^b	90.0 ^b
Δ_c^c	uÅ ²	-3.313	-3.258
N_A/N_E^d	-	138/174	117/128
σ^e	kHz	5.1	2.4

^a All parameters refer to the principal axis system. Watson's S reduction and I' representation were used. ^b Fixed due to symmetry. ^c Pseudo inertial defect. ^d Number of A and E species transitions. ^e Standard deviation of the fit.

As expected, mostly *a*- and *b*-type transitions were found for both conformers, although a small number of E-species *c*-type and *x*-type (ΔK_a and ΔK_c are both even) lines were also measured. For the E-species, the quantum numbers K_a and K_c have lost their meaning and only indicate the order of energy in analogy to the asymmetric top energy level. The rotational constant of the methyl rotor F_0 could not be fitted for either of the conformers and was fixed to 158 GHz, a typical value for methyl groups. The estimated measurement accuracy, corresponding to 1/10 of the average line width at half height, is 2.5 kHz.

3.2.2. Isotopologues

After the assignment of *syn*- and *anti*-2AT a large number of lines still remained in the spectrum which were assumed to belong to the isotopologues. With a natural abundance of 4.25% [50] ³⁴S is the isotopologue with the highest possibility to be visible in the spectrum. We first

predicted the ^{34}S frequencies for the more stable *syn*-conformer using the method explained in Ref. [51] and compared the predicted lines with those remaining in the spectrum. Straightforwardly, 51 A- and 50 E-species ^{34}S -*syn*-2AT transitions could be assigned, but the remaining unassigned lines were still numerous. Thus, we turned to the ^{13}C - and ^{18}O -isotopologue spectra. Rotational transitions of all six ^{13}C -isotopologues could be found and assigned, including A-E torsional splittings except for $^{13}\text{C}(2)$. Being close to the centre of mass of the molecule (see Figure 1), $^{13}\text{C}(2)$ transitions are close to those of the parent species and thus were often covered by the stronger main isotopologue transitions. Nevertheless, we could measure 15 transitions by exploiting that the separation between the parent species and the $^{13}\text{C}(2)$ lines increases with higher K_a quantum numbers. These transitions are weaker than those with lower K_a quantum numbers, and therefore, only A species lines could be measured, while the E species lines were too weak to be found. The ^{18}O -isotopologue spectrum was also too weak to be observed even after intensive search. The obtained molecular parameters for all *syn*-2AT isotopologues are given in Table 3, the assigned transitions of all isotopologues are listed in Table S-7 in the ESI.

Since there were still unassigned lines remaining in the spectrum, we first attempted to match them to the ^{33}S -isotopologue of *syn*-2AT with a natural abundance of 0.75%. However, the line intensities were weak due to the hyperfine splittings of the ^{33}S nucleus, and we only found a small number of possible transitions with which a reasonable fit was not achieved. We then turned to the isotopologues of *anti*-2AT and could assign the ^{34}S , $^{13}\text{C}(4)$ and $^{13}\text{C}(5)$ spectra of this conformer (see Table 4 for the fits and Table S-8 in the ESI for frequency lists), which were weak but still visible in the survey spectrum as shown in Figure 4. A small number of transitions could also be found for the other ^{13}C -isotopologues (see Table S-9), allowing initial fits using three rotational constants for $^{13}\text{C}(3)$ and $^{13}\text{C}(6)$ as given in Table S-10. We were confident that the assigned transitions belong to these isotopologues, but since further transitions were too weak to be observed and the assignment of the torsional species was uncertain, especially for the $^{13}\text{C}(3)$ isotopologue, satisfactorily accurate fits were not possible. Therefore these isotopologues are not considered further in the analysis.

3.3. Thiophene

To determine the structure of thiophene at the same quality as for 2AT for an accurate comparison, we measured the microwave spectra of thiophene as well as its ^{34}S and two ^{13}C isotopologues using the rotational constants reported in Refs. [27] and [48], respectively, as initial values. The fit results are given in Table 5; the frequency list in Table S-11.

Table 3: Molecular parameters of the ^{34}S - and ^{13}C -isotopologues of *syn*-2AT obtained with the program *XIAM*.

Par. ^a	Unit	$^{34}\text{S}(1)$	$^{13}\text{C}(2)$	$^{13}\text{C}(3)$	$^{13}\text{C}(4)$	$^{13}\text{C}(5)$	$^{13}\text{C}(6)$	$^{13}\text{C}(8)$
A_0	MHz	3526.99134(52)	3587.09861(14)	3538.0689(14)	3549.30592(91)	3588.0210(13)	3588.09149(79)	3556.6433(14)
B_0	MHz	1409.06281(21)	1415.90395(17)	1414.90446(51)	1401.38369(36)	1395.56772(42)	1405.83288(43)	1390.75940(41)
C_0	MHz	1013.51470(13)	1021.99301(19)	1017.45163(17)	1011.35655(22)	1011.42683(18)	1016.81168(28)	1006.40046(23)
D_J	kHz	0.0566(22)	0.054168 ^b	0.0476(66)	0.0565(21)	0.0584(40)	0.0528(55)	0.0550(39)
D_{JK}	kHz	0.046977 ^b	0.046977 ^b	0.046977 ^b	0.046977 ^b	0.092(30)	0.046977 ^b	0.046977 ^b
D_K	kHz	0.386(51)	0.374286 ^b	0.239(67)	0.314(73)	0.402(78)	0.482(78)	0.453(73)
d_1	kHz	-0.0180(13)	-0.017242 ^b	-0.0137(38)	-0.0173(17)	-0.0202(24)	-0.0207(29)	-0.0218(24)
d_2	kHz	-0.002231 ^b	-0.002231 ^b	-0.002231 ^b	-0.002231 ^b	-0.002231 ^b	-0.002231 ^b	-0.002231 ^b
V_3	cm^{-1}	330.069(64)	329.871494 ^b	333.48(46)	331.27(26)	329.80(13)	330.40(12)	331.52(42)
$D_{p_i^2 K}$	MHz	-0.131132 ^b	-0.131132 ^b	-0.131132 ^b	-0.131132 ^b	-0.307(49)	-0.131132 ^b	-0.131132 ^b
$\angle(i,a)$	deg	47.433(43)	52.9969 ^b	48.01(12)	48.480(72)	47.282(99)	47.918(72)	47.15(11)
$\angle(i,b)$	deg	42.567(43)	37.0031 ^b	41.99(12)	41.520(72)	42.718(99)	42.082(72)	42.85(11)
Δ_c^c	$\text{u}\text{\AA}^2$	-3.312	-3.315	-3.312	-3.313	-3.314	-3.313	-3.313
N_A/N_E^d	-	51/50	15/-	35/17	36/16	33/19	30/27	38/16
σ^e	kHz	4.4	2.3	3.5	3.7	3.6	5.3	4.2

^a All parameters refer to the principal axis system. Watson's S reduction and I^r representation were used. $\angle(i,c)$ is fixed to 90° due to symmetry in all fits. F_0 is fixed to 158.0 GHz. ^b Values of the centrifugal distortion constants and the higher order parameter $D_{p_i^2 K}$ were fixed to those of the main isotopologue given in Table 2. ^c

Pseudo inertial defect. ^d Number of A and E species transitions. ^e Standard deviation of the fit.

Table 4: Molecular parameters of the ^{34}S - and two ^{13}C -isotopologues of *anti*-2AT obtained with the program *XIAM*.

Par. ^a	Unit	$^{34}\text{S}(1)$	$^{13}\text{C}(4)$	$^{13}\text{C}(5)$
A_0	MHz	3491.23489(67)	3522.7755(17)	3554.00476(73)
B_0	MHz	1413.21114(38)	1403.58030(58)	1398.84537(48)
C_0	MHz	1012.82096(12)	1010.41239(14)	1010.49887(16)
D_J	kHz	0.0570(43)	0.05274 ^b	0.05274 ^b
D_{JK}	kHz	0.098(21)	0.0755 ^b	0.0755 ^b
D_K	kHz	0.274(54)	0.359 ^b	0.359 ^b
d_1	kHz	-0.0225(42)	-0.01719 ^b	-0.01719 ^b
d_2	kHz	-0.0064(32)	-0.002105 ^b	-0.002105 ^b
V_3	cm^{-1}	295.606(88)	/	/
$D_{p_i^2 J}$	kHz	43.22(90)	/	/
$\angle(i,a)$	deg	62.319(42)	/	/
$\angle(i,b)$	deg	27.681(42)	/	/
Δ_c^c	$\text{u}\text{\AA}^2$	-3.385	-3.354	-3.355
N_A/N_E^d	-	42/21	10/-	11/-
σ^e	kHz	2.6	1.6	3.1

^a All parameters refer to the principal axis system. Watson's S reduction and I' representation were used. $\angle(i,c)$ is fixed to 90° due to symmetry in all fits. F_0 is fixed to 158.0 GHz. ^b Values of the centrifugal distortion constants were fixed to those of the main isotopologue listed in Table 2. ^c Pseudo inertial defect. ^d Number of A and E species transitions. ^e Standard deviation of the fit.

Table 5: Experimental spectroscopic parameters of thiophene as well as its ^{34}S and two ^{13}C isotopologues obtained with the program *XIAM*. The atom numbering is given in Figure 6.

Par. ^a	Unit	main	$^{34}\text{S}(1)$	$^{13}\text{C}(2)$	$^{13}\text{C}(3)$
A_0	MHz	8041.59642(43)	8041.7155(30)	7852.7774(15)	7981.2830(11)
B_0	MHz	5418.26279(21)	5274.18524(47)	5418.40544(51)	5319.30647(34)
C_0	MHz	3235.78084(19)	3183.84324(33)	3204.80662(34)	3190.61884(22)
D_J	kHz	0.7380(56)	0.740(16)	0.746(15)	0.7190(96)
D_{JK}	kHz	0.558(12)	0.427(76)	0.488(65)	0.591(40)
D_K	kHz	1.593(12)	1.095(80)	1.62(24)	1.67(19)
d_1	kHz	-0.31584(92)	-0.3115(50)	-0.3204(55)	-0.3084(37)
d_2	kHz	-0.06484(87)	-0.0483(71)	-0.0595(60)	-0.0596(36)
Δ_c^b	$\text{u}\text{\AA}^2$	0.066	0.066	0.067	0.066
N^c	-	53	26	25	25
σ^d	kHz	1.9	2.9	3.0	2.0

^a All parameters refer to the principal axis system. Watson's S reduction and I' representation were used. ^b Pseudo inertial defect. ^c Number of transitions. ^d Standard deviation of the fit.

4. Structure determination

4.1. 2-Acetylthiophene

The *ab initio* structure of both conformers was optimized at the CCSD(T)_ae/cc-pwCVTZ level of theory. The small correction due to the basis set enlargement cc-pwCVTZ → cc-pwCVQZ was estimated at the MP2 level, and the r_e^{BO} structure was calculated using Eq. (1):

$$r_e^{BO} = r_e[\text{CCSD(T)}_{\text{ae/cc-pwCVTZ}}] + r_e[\text{MP2}_{\text{ae/cc-pwCVQZ}}] - r_e[\text{MP2}_{\text{ae/cc-pwCVTZ}}] \quad (1).$$

The accuracy of this additive method is known to be better than 0.001 Å [52], which is confirmed in the next section 4.2. where the structure of thiophene is redetermined. The final structures of 2AT are given in Table 6 and the details are in Table S-12 of the ESI.

Table 6: Equilibrium structure of 2AT (bond lengths in Å, angles in degree)

	<i>anti</i> form		[<i>syn</i> form]	
	r_e^{BOa}	$[r_e^{BOa}]$	s^b	r_e^{SE}]
S–C2	1.7225	1.7191	0.002	1.7192(17)
S–C5	1.7059	1.7063	0.002	1.70705(67)
C3–C4	1.4143	1.4159	0.002	1.41538(87)
C4=C5	1.3712	1.3708	0.002	1.3654(10)
C2–S–C5	91.990	91.574	0.3	91.404(58)
S–C5=C4	111.952	112.503	0.3	112.592(24)
C3–C4=C5	112.277	111.856	0.3	111.917(21)
C5–H9	1.0769	1.0771	0.002	1.0760(24)
S–C5–H9	120.114	120.055	0.2	120.17(24)
C4–H10	1.0786	1.0785	0.002	1.0786(24)
C5–C4–H10	124.378	124.396	0.2	124.45(23)
C3–H11	1.0787	1.0793	0.002	1.0789(24)
C4–C3–H11	125.475	124.096	0.2	124.05(24)
C2–C6	1.4790	1.4728	0.002	1.4728(19)
C6=O7	1.2150	1.2162	0.002	1.2168(17)
C6–C8	1.5076	1.5083	0.002	1.5101(11)
S–C2–C6	123.299	119.403	0.3	119.25(14)
C2–C6–O	120.167	120.832	0.3	120.17(13)
C2–C6–C8	117.774	117.130	0.3	117.63(12)
C–H _s	1.0851	1.0851	0.002	1.0846(24)
C6–C8–H _s	109.206	108.918	0.2	108.73(23)
C–H _a	1.0903	1.0897	0.002	1.0891(20)
C6–C8–H _a	110.226	110.286	0.2	109.90(19)
C2–C6–C8–H _a	59.267	59.443	0.3	59.35(21)
C2=C3	1.3742	1.3754		1.3725(18) ^c
S–C2=C3	111.006	111.450		111.50(12) ^c

^a Born-Oppenheimer r_e^{B0} structure, see Eq. (1).

^b Uncertainty used for the weighting of the predicates (preceding column).

^c Derived parameters.

As the rotational constants of all ^{13}C and the ^{34}S isotopologues of the *syn* conformer could be determined, we attempted to deduce a semiexperimental structure by fitting the equilibrium moments of inertia derived from the equilibrium rotational constants B_e

$$B_e = B_0 + \Delta B_{\text{vib}} + \Delta B_{\text{elec}} + \Delta B_{\text{cent}} \quad (2)$$

where B_0 is the experimental ground state rotational constant, ΔB_{vib} the rovibrational correction calculated from the *ab initio* cubic force field, ΔB_{cent} the centrifugal distortion correction and ΔB_{elec} the electronic correction obtained from the **g**-tensor [53]. This electronic correction has a sizable effect. Approximate values were calculated at the B3LYP-D3/6-311+G(3df,2pd) level of theory, which are $g_{aa} = -0.070$, $g_{bb} = -0.0292$ and $g_{cc} = 0.0087$, leading to the corrections $\Delta A_g = 0.137$ MHz, $\Delta B_g = 0.023$ MHz and $\Delta C_g = -0.005$ MHz. The rovibrational corrections necessary to transform the ground state rotational constants into semiexperimental equilibrium rotational constants were calculated with the B2PLYPD3/6-311+G(3df,2pd) cubic force field.

However, finally there were not enough data for a complete structure determination. Rather than fixing some parameters, the method of mixed estimation was applied [54] where the *ab initio* structure is used as supplementary data (called predicates). This method permits to determine all the structural parameters without bias and to check the compatibility of the *ab initio* structure with the semiexperimental equilibrium rotational constants (see Table S3a). The final structure is given in Table 6 together with the uncertainties used to weight the predicates (0.002 Å for the bond lengths and 0.2° or 0.3° for the bond angles). The residuals of the fit are given in Table S13. The agreement between the *ab initio* and the semiexperimental structures is reasonable. Nevertheless, there are some small but noticeable differences which may be easily explained because of small coordinates, in particular for the C2 atom with $a = -0.158$ Å and $b = 0.206$ Å, for the C5 atom with $b = -0.063$ Å and for the C6 atom with $b = -0.057$ Å.

It can be recognised from Table 6 that the structures of the *anti*- and *syn*-conformers are rather close but, for the *anti*-conformer the S–C2 bond is longer by 0.003 Å and the C2–C6 bond is longer by 0.006 Å. Moreover, the bond angle S–C2–C6 is 3.9° larger and the C4–C3–H11 angle 1.3° larger.

4.2. Thiophene

In order to compare the structure of the ring of 2AT with that of thiophene, the equilibrium structure of the latter molecule was redetermined. The substitution structure (r_s) of thiophene was reported first in 1961 by Bak et al. [27], as given in Table 7, and also by gas-phase electron diffraction [55,56]. Later, the zero-point average r_α structure was obtained by a combined analysis of electron diffraction, liquid crystal NMR and rotational data [57]. The semi-experimental equilibrium structure r_e determined from electron diffraction data in combination with experimental rotational constants and *ab initio* force field [58] is also shown in Table 7. Quite recently, Penocchio et al. reported the r_e^{SE} structure derived from microwave data using a cubic force field of B2PLYP/cc-pVTZ quality [59], see Table 7. Although the last structure is precise, it was calculated using the ground state rotational constants reported by Bak et al. in 1961, which are not accurate. It is known that the quality of the structural fit is sensitive to the accuracy of the ground state rotational constants in use [60]. For this reason, we remeasured the microwave spectra of the ^{13}C and ^{34}S isotopologues in the present work to obtain experimental rotational constants with the same accuracy as those of 2AT. A comparison of the final results are visualised in Figure 6.

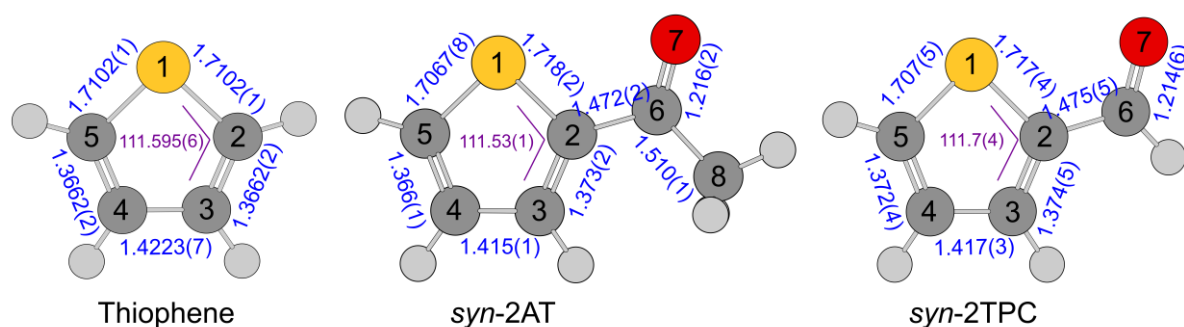


Figure 6: Comparison of the r_e^{SE} $\angle(\text{S1}-\text{C2}=\text{C3})$ angle (purple, in degrees) and bond lengths (blue, in Å) of thiophene (this work), *syn*-2AT (this work) and the *syn*-conformer of 2-thiophenecarboxaldehyde (2TPC) [61].

To further improve the accuracy, the frequencies of all isotopologues were fitted using the same number of centrifugal distortion constants. When one such constant is not experimentally determined, the method of predicate observations was employed [54]. Approximate values (predicates) for the undetermined constants were obtained from the *ab initio* force field and were scaled using the constants of the parent species. These predicates were entered as additional data in the fit with an uncertainty of 10% of their value. An analysis of residuals was then performed to check the compatibility of all data. This method significantly improves the accuracy of the rotational constants. For example, the previous *A* rotational

constant of the $^{13}\text{C}(2)$ isotopologue was 7852.89 MHz whereas the new one is 7852.77596(7) MHz. For the deuterated species, the constants of Bak et al. [27] were used but with a much lower weight.

A new cubic force field was also calculated at the B2PLYP-D3 level of theory using the Pople 6-311+G(3df,2pd) basis set. This latter basis set usually gives results close to the cc-pVTZ one. In particular, it delivers slightly more accurate bond angles and should perform better in the presence of sulphur [62]. The quality of this choice in basis set is confirmed by the extremely small value of $0.00008 \text{ u}\text{\AA}^2$ of the equilibrium inertial defect Δ_e . The results of the new fit are given in Table 7 where they are compared to the previous results. Two differences are noticeable. On the one hand, the $r(\text{C-S})$ bond length at $1.7102(1) \text{ \AA}$ is slightly shorter than the value of $1.7126(5) \text{ \AA}$ from Penocchio et al. [59]. On the other hand, the $r(\text{C2=C3})$ bond length at $1.3663(2) \text{ \AA}$ is longer than the previous value of $1.3622(8) \text{ \AA}$. These differences are explained by a better accuracy of the rotational constants.

To check the accuracy of the semiexperimental structure, we performed optimizations at the CCSD(T) level of theory, all electrons being correlated using Equation (1), but also at the CCSD(T)_ae/cc-pwCVQZ level, as given Table 7. The agreement is quite satisfactory even for the value of the $r(\text{C-S})$ bond which is 1.7116 \AA with the approximate method (Eq. 1) and 1.7107 \AA with the cc-pwCVQZ basis set. We thus conclude that the accuracy of the approximate method is about 0.001 \AA for the C-S bond and confirm the assumption taken for 2AT. We also note that the equilibrium rotational constants derived from the CCSD(T)_ae/cc-pwCVQZ structure are quite close to the corresponding semiexperimental values. For the parent species, the values obtained at the CCSD(T)_ae/cc-pwCVQZ level are $A_e = 8100.95 \text{ MHz}$, $B_e = 5446.50 \text{ MHz}$ and $C_e = 3256.84 \text{ MHz}$, to be compared with $A_e^{\text{SE}} = 8103.07 \text{ MHz}$, $B_e^{\text{SE}} = 5449.19 \text{ MHz}$ and $C_e^{\text{SE}} = 3258.36 \text{ MHz}$, i.e. deviating by only up to 0.05%.

After the completion of our work, a new semiexperimental structure of thiophene was published [63] which we also listed in Table 7. This new structure was obtained with the help of accurate ground state rotational constants of 24 isotopologues and a rovibrational correction calculated at the CCSD(T)/cc-pCVTZ level of theory. The comparison of the different structures is interesting. Firstly, the structure reported by Orr et al. [63] is in very good agreement with our r_e^{SE} structure, confirming the fact that it is essential to use accurate ground state rotational constants and that the structures of relatively rigid molecules are not sensitive to systematic errors of the rovibrational corrections [64]. Whereas the general agreement is rather pleasing, there are small differences of about 0.0008 \AA between the most accurate structure BTE (best theoretical estimate) in Table 7 and the r_e^{SE} structure determined in Orr et al. [63] for the C2-H2 and C2-C3 bond lengths. These differences, although small, are larger than the standard deviations of the parameters. It is an indication that the standard deviations are probably not a

reliable indicator of the accuracy because they do not take into account the systematic errors, mainly due to the poor conditioning of the system of normal equations and the presence of very small coordinates (in the case of thiophene, $a(\text{C2}) = 0.046 \text{ \AA}$ and $a(\text{H2}) = -0.253 \text{ \AA}$) [52].

Table 7: Structures of thiophene (bond lengths in Å, angles in degree).

Method	r_s	ED + MW ^a		r_e^{SE}		CCSD(T)_ae		BTE ^a
Ref.	Bak 61 ²⁷	Kochikov ⁵⁸	Penocchio ⁵⁹	This work	Orr ⁶³	cc-pwCVQZ	Eq. (1)	Orr ⁶³
C-S	1.7140(14)	1.704(2)	1.7126(5)	1.71023(11)	1.7105(1)	1.7107	1.7116	1.7103
C2-H2	1.0776(15)	1.085(5)	1.0771(5)	1.07667(50)	1.0771(1)	1.0764	1.0763	1.0764
S-C-H2	119.85(78)	119.9(3)	120.11(10)	120.203(97)	120.065(14)	120.288	120.272	120.241
C2=C3	1.3696(17)	1.372(3)	1.3622(8)	1.36625(17)	1.3656(2)	1.3665	1.3668	1.3666
S-C2=C3	111.47(23)	111.6	111.66(3)	111.5951(58)	111.608(8)	111.611	111.625	111.610
C3-H3	1.0805(14)	1.088	1.0794(3)	1.07838(21)	1.0786(1)	1.0787	1.0787	1.0787
C2=C3-H3	123.25(7)	123.4	123.46(3)	123.459(15)	123.414(12)	123.416	123.421	123.411
C-S-C	92.17(10)	92.4(2)	91.88(4)	92.0787(82)	92.047(8)	92.059	92.027	92.072

^a Electron diffraction combined with microwave spectroscopy data. ^b Best theoretical estimate.

5. Discussion

5.1. Conformational stability

Quantum chemical calculations at different levels of theory consistently predict the *syn*-conformer of 2AT to be energetically more stable than the *anti*-conformer. However, the difference in energy varies strongly from about 2.1 to 6.2 kJ·mol⁻¹ (see Table S-3 of the ESI). The relative intensity observed in the experimental spectrum indicates that transitions of the *anti*-conformer are only slightly weaker than those of the *syn* form, as can be recognised exemplarily for the *a*-type transition 4₀₄ ← 3₀₃ in Figure 4 as well as the *b*-type transition 5₀₅ ← 4₁₄ in Figure S-1 in the ESI, hinting at a rather small energy difference. Nevertheless, we do not attempt to provide a quantitative statement on the conformational stability and intensity due to the lack of dipole moment measurements and the trust in intensity ratio obtained with the experimental setups in use.

The microwave spectra of two other thiophene derivatives related to 2AT (molecule **(2)** in Figure 7), 2-thiophenecarboxaldehyde (**(1)**) [61] and 2-acetyl-3-methylthiophene (**(3)**) [65], have been reported in the literature. All three molecules exhibit two stable conformers with the S–C bond and the carbonyl group in *anti* or *syn* position, with the *syn*-conformer being more stable (see Figure 7). Compared to the observation found for 2-acetylfuran (**(5)**) and its related molecules furfural (**(4)**) [66], methyl furfural [67] and 2-acetyl-5-methylfuran (**(6)**) [68], we found that the heteroatom in the ring significantly affects the conformational stability. The *syn*-conformer of 2-acetylfuran is much higher in energy than the *anti*-conformer [10]. Obviously, changing oxygen by sulphur reverses the conformational stability. A reason for the preference of one form (*syn* or *anti*) may be the different electrostatic interaction between the oxygen atom of the carbonyl group and the sulphur in the thiophene ring of 2AT or the oxygen atom in the furan ring of 2-acetylfuran. The negative charges on the oxygen atoms of 2-acetylfuran stabilises the *anti*-conformer [10], while the *syn*-form is favored by the opposite charges on the oxygen and sulphur atoms in 2AT, as visualised also in Figure 8 with the charge data obtained from NBO calculations [32].

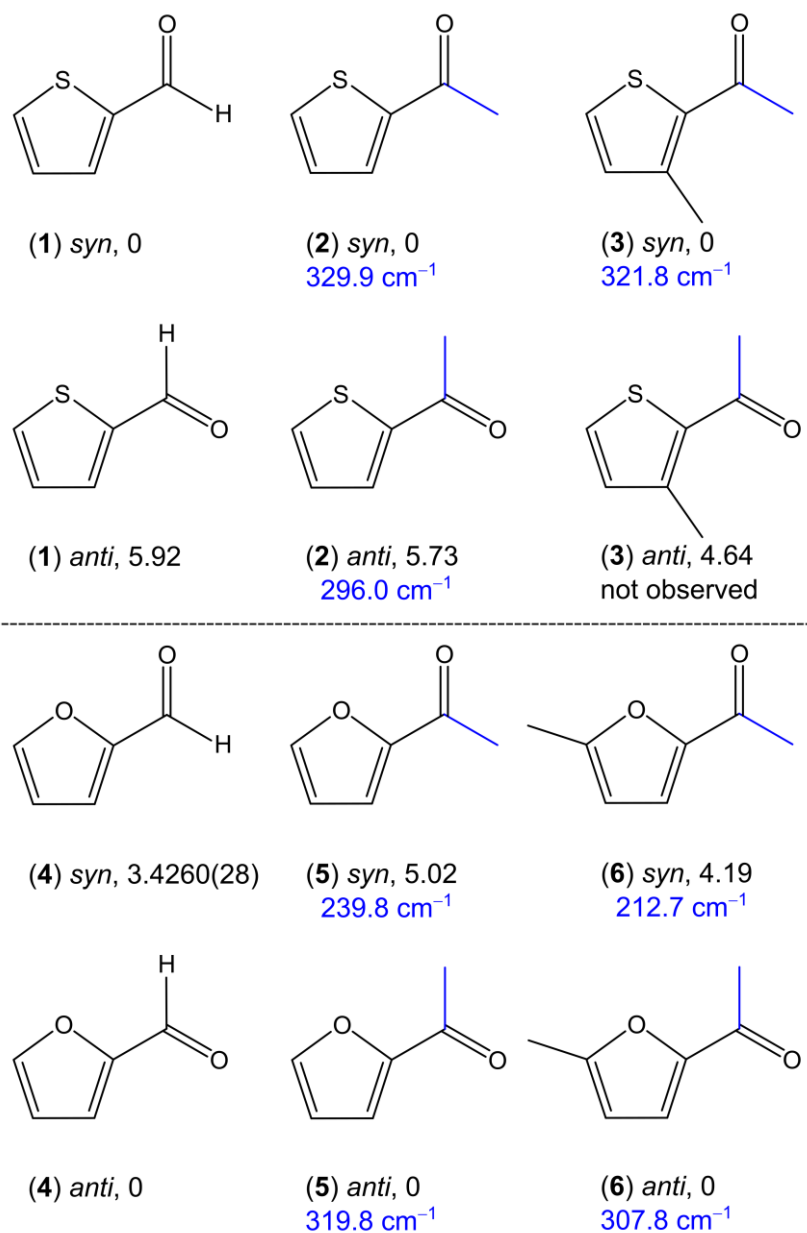


Figure 7: Thiophene and furan derivatives with a carboxaldehyde or an acetyl substitution at the second ring position: (1) 2-Thiophenecarboxaldehyde [61], (2) 2-acetylthiophene (this work), (3) 2-acetyl-3-methylthiophene [65], (4) furfural [66], (5) 2-acetylfuran [10] and (6) 2-acetyl-5-methylfuran [68]. For each molecule, the *syn*- and *anti*-conformers are illustrated with their energy (in kJ·mol⁻¹) relative to the more stable conformer. The torsional barrier of the acetyl methyl group is also given.

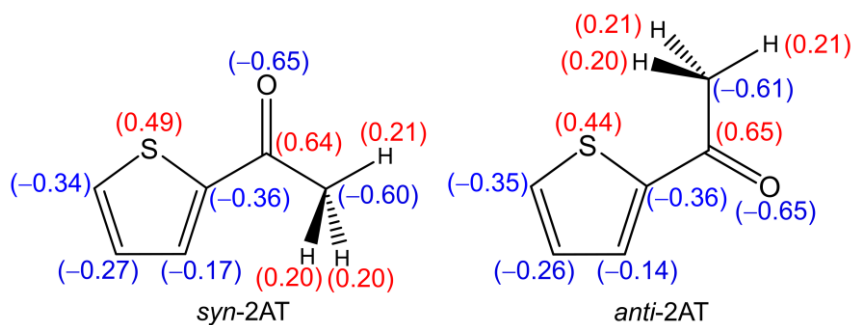


Figure 8: Charge distribution in *syn*- and *anti*-2AT obtained from NBO calculations at the MP2/6-311++G(d,p) level of theory.

5.2. Quality of the fits

As can be recognised in Table 2, using three rotational constants, five quartic centrifugal distortion constants, the angle between the internal rotor axis and the principal *a*-axis, as well as two higher order parameters $D_{p_i^2 J}$ and $D_{p_i^2 K}$, describing the centrifugal distortion of the methyl internal rotor, the standard deviation achieved for *anti*-2AT is 2.4 kHz, which is the measurement accuracy. For *syn*-2AT, if the $D_{p_i^2 J}$ parameter is included, the standard deviation of the fit is 1.9 kHz, showing that the *XIAM* program performs well for both conformers of 2AT. However, the *A* rotational constant strongly correlates with $D_{p_i^2 J}$. By fitting $D_{p_i^2 J}$, we found that for the main isotopologue of *syn*-2AT, (i) the *A* rotational constant is by two orders of magnitude less well-determined and (ii) its value changes by 1.6 MHz, as summarised in Table 8. Interestingly, the fits of all isotopologues, except C(2) for which no E species lines are observable, are much less sensitive to $D_{p_i^2 J}$, so that the two above mentioned problems do not occur. In order to get a good set of rotational constants for structure determination purpose, we decided not to fit $D_{p_i^2 J}$ to decrease the correlation of the *A* rotational constant, as well as increase its accuracy. As a consequence, we only achieve a standard deviation of 5.1 kHz, two times the measurement accuracy. All *syn*-2AT isotopologue fits possess a standard deviation close to this value (except $^{13}\text{C}(2)$ with a much better deviation of 2.3 kHz due to the observation of only A species lines). We note that if only A species lines are available, reliable rotational constants for structure determination purposes can still be obtained by fixing all internal rotation parameters to those of the parent species.

Table 8: Rotational constants, higher order $D_{p_i^2 J}$ and $D_{p_i^2 K}$ parameters, standard deviation σ and pseudo inertial defect Δ_c of *syn*- and *anti*-2AT obtained with the program XIAM using different sets of high order parameters.

Par.	Unit	<i>syn</i> -2AT				<i>anti</i> -2AT			
		$D_{p_i^2 J} + D_{p_i^2 K}$	$D_{p_i^2 J}$	$D_{p_i^2 K}^a$	none	$D_{p_i^2 J} + D_{p_i^2 K}^b$	$D_{p_i^2 J}$	$D_{p_i^2 K}$	none
A	MHz	3589.676(26)	3588.04877(38)	3588.05339(29)	3588.04887(38)	3555.438(21)	3554.61453(75)	3554.6181(11)	3554.6155(11)
B	MHz	1415.7100(49)	1415.91824(20)	1415.91822(11)	1415.91833(19)	1418.7605(47)	1419.16713(28)	1419.16865(34)	1419.16879(36)
C	MHz	1021.8664(49)	1022.07432(14)	1022.074502(72)	1022.07440(13)	1020.7702(47)	1021.17627(20)	1021.17725(25)	1021.17724(26)
$D_{p_i^2 J}$	kHz	19.73(46)	2.9(19)	/	/	41.06(48)	28.7(19)	/	/
$D_{p_i^2 K}$	MHz	-0.1739(22)	/	-0.1311(53)	/	-0.1239(19)	/	-0.0580(99)	/
σ	kHz	1.9	8.8	5.1	8.8	2.4	10.5	13.9	14.9
Δ_c^c	uÅ ²	-3.201	-3.313	-3.313	-3.313	-3.258	-3.386	-3.386	-3.386

^a Fit chosen for structure determination as given in Table 2. ^b Fit given in Table 2.

5.3. Rotational constants

Values of equilibrium rotational constants of *syn*-2AT calculated at different levels of theory summarised in Tables S3 are generally close to those deduced from the experiments at basis sets using the (ndf,npd) polarization functions ($n = 1-3$) in combination with the MP2 or B3LYP methods. For the M06-2X and ω B97XD methods, the 6-311G(d,p) basis set with or without diffuse functions performs well. In the case of *anti*-2AT, only the three levels M06-2X/6-311G(d,p), M06-2X/6-311+G(d,p) and M06-2X/6-311++G(d,p) seem to work well. This is not the same finding as for the furan analogue 2-acetylfuran where the three B3LYP-D3BJ/6-311(++G(d,p) levels are recommended. Obviously, furan and thiophene derivatives require different error compensations to access reliable starting values of the rotational constants to guide the spectral assignment. We note that, certainly, the equilibrium rotation constants of CCSD(T)_ae/cc-pwCVQZ quality derived for the r_e^{BO} structures possess the highest accuracy, but these costly calculations are worthwhile to evaluate the structure determination rather than at the assignment step.

The rotational constants obtained from global fits with the program *XIAM* are suitable for a high quality structure determination of 2AT, which is also the case of the oxygen analogue 2-acetylfuran [10]. However, special attentions are needed if higher order parameters such as $D_{p_i^2 J}$, $D_{p_i^2 K}$ and $D_{p_i^2 -}$ are involved, as they are often highly correlated with A , B and C . It is therefore recommended to check the consistency of the pseudo inertial defects (see Tables 2, 3 and 4), whose values should remain almost the same for the main species and all isotopologues. We note at this point that for *anti*-2AT, fitting both the $D_{p_i^2 J}$ and $D_{p_i^2 K}$ parameters is decisive to achieve a good fit with standard deviation within the measurement accuracy (see Table 8). But similar to the case of *syn*-2AT, the rotational constants, especially A , but also B and C , suffer from correlations and are not as well-determined as when either $D_{p_i^2 J}$ or $D_{p_i^2 K}$ or none of them are fitted. The pseudo inertial defect of $-3.258 \text{ u}\text{\AA}^2$ of Fit $D_{p_i^2 J} + D_{p_i^2 K}$ in Table 8 differs significantly to the value of $-3.386 \text{ u}\text{\AA}^2$ found for the other fit, which is essentially similar to that of the ^{34}S -*anti*-2AT fit given in Table 4. Since the r_e^{SE} structure of *anti*-2AT cannot be determined, we decided to fit both $D_{p_i^2 J}$ and $D_{p_i^2 K}$ to obtain a low standard deviation. For structure determination purpose, rotational constants from Fit $D_{p_i^2 J}$ of *anti*-2AT should be used.

5.4. Molecular geometries

For an accurate comparison, it is important that the structures in use have the same physical meaning. As thiophene derivatives, only the r_e^{SE} structures of *syn*-2AT (this work) and *syn*-2-thiophenecarboxaldehyde [61] are available in the literature. Comparing thiophene with 2AT (see Figure 6), we found that the C4=C5 bond length is the same in both molecules. On the

other hand, the $\angle(\text{S1}-\text{C2}=\text{C3})$ angle at the substitution position of *syn*-2AT is smaller, making the S1–C2 and C2=C3 bonds longer as well as the S1–C5 and C3–C4 bonds shorter. Though the r_e^{SE} structure of 2-thiophenecarboxaldehyde [61] is not determined at the same quality and the large error of the $\angle(\text{S1}-\text{C2}=\text{C3})$ angle inhibits a reasonable comparison, the bond lengths of 2-thiophenecarboxaldehyde suggest the same trend. The C2–C6 and C6=O7 bonds of *syn*-2AT and 2-thiophenecarboxaldehyde are in extremely good agreement, showing the rigidity of the carbonyl moiety.

Comparing the structure of thiophene with that of furan, as well as 2AT vs 2-acetylfuran, we found that in the hetero-atom rings, only the C3–C4 bond length is longer in furans (by about 0.01 Å). The C2=C3 and C4=C5 bonds in thiophenes are 0.01 Å longer. Because sulphur is much larger than oxygen, the S–C bonds are 0.35 Å longer than the O–C bonds and the $\angle(\text{S}-\text{C}=\text{C})$ angle is about 1° larger than the $\angle(\text{O}-\text{C}=\text{C})$ angle.

Most of the structure computations at different levels of theory (see Tables S-3a and S-3b in the ESI) predicted symmetric equilibrium configuration with C_s point-group symmetry for each of the two 2AT conformers. Vibrational frequency calculations at most levels did not yield imaginary frequencies and thus confirmed that optimized structures correspond to real minima. Following to these predictions, the structure optimizations at the CCSD(T) level of theory were carried out for the symmetric configurations.

According to results of the MP2/6-311++G(d,p) calculations, the *anti*-2AT conformer has two non-symmetric equilibrium configurations (C_1 point-group symmetry) with the angle α deviating from 180° by about 6° (called the tilt angle Θ , see Table S-3b) corresponding to the double minimum potential shown in Figure 2. This behaviour of the MP2/6-311++G(d,p) approximation was frequently observed in ketones, such as *n*-alkyl ketones [4-7], 2-propionylthiophene [51], 2-acetyl-3-methylthiophene [65], pinacolone [69], and diethyl ketone [70]. However, since the barrier between these configurations is not significant (essentially lower than the first vibrational state), the S(1)–C(2)–C(6)=O(7) fragment should be considered as quasi-planar in this particular prediction. This is supported experimentally by the pseudo inertial defect of *anti*-2AT given in Table 4.

5.5. Methyl internal rotation

The torsional barrier of the acetyl methyl group could be well-determined in the fits of both conformers and most of the observed isotopologues. Only for C(2)-*syn*-2AT which lies almost at the center of mass of the molecule and the two ^{13}C isotopologues observable for *anti*-2AT, no E species transitions were measurable and therefore, the torsional barrier could not be deduced. For *syn*-2AT, we found a barrier height of about 329.9 cm^{-1} for the parent

species, which remains almost constant for all isotopologues and very close to the value of 321.8 cm^{-1} found for the *syn* conformer of 2-acetyl-3-methylthiophene [65] (see Figure 7). A slightly lower, yet similar value of about 296 cm^{-1} was obtained for *anti*-2AT as well as its ^{34}S isotopologue. Concerning the establishment of a possible “thiophene class” in the categorization of ketones containing an acetyl methyl group [7,9], the results obtained from 2AT are very promising. However, since there are currently only two data points, 2AT and 2-acetyl-3-methylthiophene [65], where the *anti*-conformer is not observable in the latter molecule, a conclusive classification is not attempted at this stage.

We observed the contrary in the oxygen analogue of 2AT where the torsional barrier of *anti*-2-acetylfuran (319.8 cm^{-1}) is higher than that of *syn*-2-acetylfuran (239.8 cm^{-1}) [10], which is also the case of 2-acetyl-5-methylfuran (307.8 cm^{-1} vs 212.7 cm^{-1}) [68]. The more stable conformer seems to possess a higher barrier to internal rotation of the acetyl methyl group. From the discussion on conformational stability, this supports our suspicion that electrostatic interaction plays an important role for the acetyl methyl torsion.

Comparing the barrier height of *syn*-2AT and *syn*-2-acetylfuran (329.9 cm^{-1} vs. 239.8 cm^{-1}) as well as *anti*-2AT and *anti*-2-acetylfuran (296.0 cm^{-1} vs. 319.8 cm^{-1}), we surprisingly found that for the *syn*-conformers, the higher torsional barrier is observed for the sulphur analogue, in contrast to the frequent observation that the torsional barriers of methyl internal rotors in oxygen analogues are higher, which maintains true for the *anti*-conformer. We have no explanation for this strange observation, but again suspect electrostatic effects to be the reason.

6. Conclusion

The *syn*- and *anti*-conformers were assigned in the microwave spectrum of 2AT, as well as the ^{34}S -isotopologue, all ^{13}C -isotopologues of *syn*-2AT and some ^{13}C -isotopologues of *anti*-2AT, to gain insights in two subjects: (i) methyl internal rotation and (ii) structure determination. (i) A-E splittings could be resolved for the main isotopologues of *syn*- and *anti*-2AT, as well as for the ^{34}S -isotopologue of *anti*-2AT and all isotopologues of *syn*-AT except $^{13}\text{C}(2)$ which lies almost at the centre of mass. Analysing these splittings enables the determination of a torsional barrier of about 296 cm^{-1} for *anti*-2AT and 330 cm^{-1} for *syn*-2AT, whereby the latter is surprisingly higher than the values of *syn*-2-acetylfuran. (ii) Comparing the r_e^{SE} structure of 2AT with that of thiophene, we found that the presence of an acetyl substituent increases the S1–C2 and C2=C3 bond lengths of thiophene, as well as decreases the bond angle S1–C2=C3. Comparison of thiophene vs furan and 2AT vs 2-acetylfuran leads to the conclusion that the C3–C4 bond length is about 0.01 \AA longer in furans, the C2=C3 and C4=C5 bonds are 0.01 \AA

longer in thiophenes, the S–C bond lengths are 0.35 Å longer than the O–C ones and the S–C=C angle is about 1° larger than the O–C=C angle.

Acknowledgments

This work was supported by the Agence Nationale de la Recherche ANR (project ID ANR-18-CE29-0011) and by the Dr. B. Mez-Starck Foundation (Germany). A part of the simulations was performed with computing resources granted by the RWTH Aachen University under the project rwth0369.

References

- [1] D. G. Lister, J. N. MacDonald and N. L. Owen in *Internal Rotation and Inversion: An Introduction to Large Amplitude Motions in Molecules* Academic Press, New York, **1978**.
- [2] H. V. L. Nguyen and I. Kleiner in *Theoretical and computational chemistry*, (Eds. I. Gulaczyk, B. Tylkowski), De Gruyter, Berlin/Boston, **2021**, pp. 41-78.
- [3] H. Dreizler, *Z. Naturforsch.*, 1961, **16a**, 1354.
- [4] M. Andresen, I. Kleiner, M. Schwell, W. Stahl and H. V. L. Nguyen, *J. Phys. Chem. A.*, 2018, **122**, 7071.
- [5] M. Andresen, I. Kleiner, M. Schwell, W. Stahl and H. V. L. Nguyen, *ChemPhysChem*, 2019, **20**, 2063.
- [6] M. Andresen, I. Kleiner, M. Schwell, W. Stahl and H. V. L. Nguyen, *J. Phys. Chem. A.*, 2020, **124**, 1353.
- [7] M. Andresen, M. Schöngen, I. Kleiner, M. Schwell, W. Stahl and H. V. L. Nguyen, *ChemPhysChem*, 2020, **21**, 2206.
- [8] S. Herbers, S. M. Fritz, P. Mishra, H. V. L. Nguyen and T. S. Zwier, *J. Chem. Phys.*, 2020, **152**, 074301.
- [9] M. Andresen, M. Schwell and H. V. L. Nguyen, *J. Mol. Struct.*, 2021, **1247**, 131337.
- [10] C. Dindić, A. Lüchow, N. Vogt, J. Demaison and H. V. L. Nguyen *J. Phys. Chem. A.*, 2021, **125**, 4986.
- [11] A. Jabri, V. Van, H. V. L. Nguyen, H. Mouhib, F. Kwabia-Tchana, L. Manceron, W. Stahl and I. Kleiner, *Astron. Astrophys.*, 2016, **589**, A127.
- [12] W. Neustock, A. Guarnieri, J. Demaison and G. Wlodarczak, *Z. Naturforsch.*, 1990, **45a**, 702.

- [13] A. Jabri, B. Tercero, L. Margulès, R. A. Motiyenko, E. A. Alekseev, I. Kleiner, J. Cernicharo and J.-C. Guillemin, *Astron. Astrophys.*, 2020, **644**, A102.
- [14] M. Carvajal, F. Willaert, J. Demaison and I. Kleiner, *J. Mol. Spectrosc.*, 2007, **246**, 158.
- [15] N. M. Pozdeev, L. N. Gunderova and A. A. Shapkin, *Opt. Spectrosc.* 1970, **28**, 254.
- [16] W. G. Norris and L. C. Krisher, *J. Chem. Phys.*, 1969, **51**, 403.
- [17] T. Ogata and K. Kozima, *J. Mol. Spectrosc.*, 1972, **42**, 38.
- [18] T. Ogata and K. Kozima, *Bull. Chem. Soc. Jpn.*, 1971, **44**, 2344.
- [19] V. Van, W. Stahl and H. V. L. Nguyen, *Phys. Chem. Chem. Phys.*, 2015, **17**, 32111.
- [20] V. Van, J. Bruckhuisen, W. Stahl, V. Ilyushin and H. V.L. Nguyen, *J. Mol. Spectrosc.* 2018, **343**, 121.
- [21] J. Demaison, H. D. Rudolph, A. G. Császár, *Mol. Phys.*, 2013, **111**, 9.
- [22] H. D. Rudolph, J. Demaison, A. G. Császár, *J. Phys. Chem. A* 2013, **117**, 12969.
- [23] N. Vogt, I. I. Marochkin, A. N. Rykov, O. V. Dorofeeva, *J. Phys. Chem. A* 2013, **117**, 11373.
- [24] N. Vogt, I. I. Marochkin, A. N. Rykov, *J. Phys. Chem. A* 2015, **119**, 152.
- [25] N. Vogt, I. I. Marochkin, A. N. Rykov, *Phys. Chem. Chem. Phys.* 2018, **20**, 9787.
- [26] B. Bak, D. Christensen, J. Rastrup-Andersen and E. Tannanbaum, *J. Chem. Phys.*, 1956, **25**, 892.
- [27] B. Bak, D. Christensen, L. Hansen-Nygaard, J. Rastrup-Andersen, *J. Mol. Spectrosc.*, 1961, **7**, 58.
- [28] C. Møller, M.S. Plesset, *Phys. Rev.*, 1934, **46**, 618-622.
- [29] A.D. Becke, *J. Chem. Phys.* 1993, **98**, 5648–5652.
- [30] C. Lee, W. Yang, R.G. Paar, *Phys. Rev. B* 1988, **37**, 785–789.
- [31] M.J. Frisch, J.A. Pople, J.S. Binkley, *J. Chem. Phys.* 1984, **80**, 3265-3269.
- [32] M. J. Frisch, G. W. Trucks, H. B. Schlegel, G. E. Scuseria, M. A. Robb, J. R. Cheeseman, G. Scalmani, V. Barone, G. A. Petersson, H. Nakatsuji, X. Li, M. Caricato, A. V. Marenich, J. Bloino, B. G. Janesko, R. Gomperts, B. Mennucci, H. P. Hratchian, J. V. Ortiz, A. F. Izmaylov, J. L. Sonnenberg, D. Williams-Young, F. Ding, F. Lipparini, F. Egidi, J. Goings, B. Peng, A. Petrone, T. Henderson, D. Ranasinghe, V. G. Zakrzewski, J. Gao, N. Rega, G. Zheng, W. Liang, M. Hada, M. Ehara, K. Toyota, R. Fukuda, J. Hasegawa, M. Ishida, T. Nakajima, Y. Honda, O. Kitao, H. Nakai, T. Vreven, K. Throssell, J. A. Montgomery, Jr., J. E. Peralta, F. Ogliaro, M. J. Bearpark, J. J. Heyd, E. N. Brothers, K. N. Kudin, V. N. Staroverov, T. A. Keith, R. Kobayashi, J. Normand, K. Raghavachari, A. P.

- Rendell, J. C. Burant, S. S. Iyengar, J. Tomasi, M. Cossi, J. M. Millam, M. Klene, C. Adamo, R. Cammi, J. W. Ochterski, R. L. Martin, K. Morokuma, O. Farkas, J. B. Foresman and D. J. Fox, *Gaussian 16, Revision B.01*, Gaussian, Inc., Wallingford CT, 2016.
- [33] S. Grimme, *J. Comput. Chem.*, 2006, **27**, 1787.
- [34] S. Grimme, S. Ehrlich, L. Goerigk, *J. Comput. Chem.* 2011, **32**, 1456-1465.
- [35] H.V.L. Nguyen and W. Stahl, *ChemPhysChem*, 2011, **12**, 1900.
- [36] I. Uriarte, A. Insausti, E. J. Cocinero, A. Jabri, I. Kleiner, H. Mouhib, I. Alkorta, *J. Phys. Chem. Lett.*, 2018, **9**, 5906.
- [37] Y. Zhao, D.G. Truhlar, *Theor. Chem. Acc.* 2008, **120**, 215-241.
- [38] J.-D. Chai, M. Head-Gordon, *Phys. Chem. Chem. Phys.* 2008, **10**, 6615-6620.
- [39] G. D. Purvis III and R. J. Bartlett, *J. Chem. Phys.*, 1982, **76**, 1910.
- [40] K. Raghavachari, G. W. Trucks, J. A. Pople and M. A Head-Gordon, *Chem. Phys. Lett.*, 1989, **157**, 479.
- [41] K. A. Peterson and T. H. Dunning Jr. *J. Chem. Phys.*, 2002, **117**, 10548.
- [42] S. Grimme, *J. Chem. Phys.*, 2006, **124**, 034108.
- [43] H.-J. Werner, P. J. Knowles, G. Knizia, F. R. Manby and M. Schütz, *WIREs* 2012, **2**, 242. MOLPRO, version 2019.2, a package of ab initio programs, H.-J. Werner, P. J. Knowles, G. Knizia, F. R. Manby, M. Schütz, P. Celani, W. Györfy, D. Kats, T. Korona, R. Lindh, A. Mitrushenkov, G. Rauhut, K. R. Shamasundar, T. B. Adler, R. D. Amos, S. J. Bennie, A. Bernhardsson, A. Berning, D. L. Cooper, M. J. O. Deegan, A. J. Dobbyn, F. Eckert, E. Goll, C. Hampel, A. Hesselmann, G. Hetzer, T. Hrenar, G. Jansen, C. Köppl, S. J. R. Lee, Y. Liu, A. W. Lloyd, Q. Ma, R. A. Mata, A. J. May, S. J. McNicholas, W. Meyer, T. F. Miller III, M. E. Mura, A. Nicklass, D. P. O'Neill, P. Palmieri, D. Peng, K. Pflüger, R. Pitzer, M. Reiher, T. Shiozaki, H. Stoll, A. J. Stone, R. Tarroni, T. Thorsteinsson, M. Wang and M. Welborn, see <https://www.molpro.net>.
- [44] H.-J. Werner, P. J. Knowles, G. Knizia, F. R. Manby and M. Schütz, *WIREs Comput. Mol. Sci.* 2012, **2**, 242.
- [45] J.-U. Grabow, W. Stahl and H. Dreizler, *Rev. Sci. Instrum.*, 1996, **67**, 4072.
- [46] I. Merke, W. Stahl, H. Dreizler, *Z. Naturforsch.* 1994, **49a**, 490.
- [47] J.-U. Grabow and W. Stahl, *Z. Naturforsch.*, 1990, **45a**, 1043.
- [48] U. Kretschmer, W. Stahl and H. Dreizler, *Z. Naturforsch.*, 1993, **48a**, 733.

- [49] H. Hartwig and H. Dreizler, *Z.Naturforsch.*, 1996, **51a**, 923.
- [50] M. Berglund and M. E. Wieser, *Pure Appl. Chem.*, 2011, **83**, 397.
- [51] C. Dindić, W. Stahl and H. V. L. Nguyen, *Phys. Chem. Chem. Phys.*, 2020, **22**, 19704.
- [52] J. Demaison, N. Vogt, *Accurate structure determination of free molecules*, Springer **2020**.
- [53] D. H. Sutter and W. H. Flygare, *J. Am. Chem. Soc.*, 1969, **91**, 4063.
- [54] J. Demaison, J. E. Boggs, A. G. Csaászár, *The Method of Least Squares. In Equilibrium Molecular Structures*; Eds.; CRC Press: Boca Raton, FL, **2011**.
- [55] R. A. Bonham and F. A. Momany, *J. Phys. Chem.*, 1963, **67**, 2474.
- [56] W. R. Harschbarger and S. H. Bauer, *Acta Cryst.*, 1970, **B26**, 1010.
- [57] Lischeski JMSt 186 (1988) 227.
- [58] I. V. Kochikov, Y. I. Tarasov, V. P. Spiridonov, G. M. Kuramshina, D. W. H. Rankin, A. S. Saakjan and A. G. Yagola, *J. Mol. Struct.*, 2001, **567-568**, 29.
- [59] E. Penocchio, M. Piccardo and V. Barone, *J. Chem. Theory Comput.*, 2015, **11**, 4689.
- [60] H. D. Rudolph, J. Demaison and A. G. Császár, *J. Phys. Chem. A.*, 2013, **117**, 12969.
- [61] R. Hakiri, N. Derbel, W. C. Bailey, H. V. L. Nguyen and H. Mouhib, *Mol. Phys.*, 2020, **118**, e1728406.
- [62] J. M. L. Martin and O. Uzan, *Chem Phys. Lett.*, 1998, **282**, 16.
- [63] V.L. Orr, Y. Ichikawa, A.R. Patel, A.M. Kougias, K. Kobayashi, J.F. Stanton, B.J. Esselman, R.C. Woods and R. J. McMahon, *J. Chem. Phys.*, 2021, **154**, 244310.
- [64] N. Vogt, J. Demaison, J. Vogt, H. D. Rudolph, *J. Comput. Chem.* 2014, **35**, 2333.
- [65] C. Dindić and H.V.L. Nguyen, *ChemPhysChem*, 2021, DOI: 10.1002/cphc.202100514
- [66] R. A. Motiyenko, E. A. Alekseev, S. F. Dyubko and F. J. Lovas, *J. Mol. Spectrosc.*, 2006, **240**, 93.
- [67] R. Hakiri, N. Derbel, H. V. L. Nguyen and H. Mouhib, *Phys. Chem. Chem. Phys.*, 2018, **20**, 25577.
- [68] V. Van, W. Stahl and H. V. L. Nguyen, *ChemPhysChem.*, 2016, **17**, 3223.
- [69] Y. Zhao, H.V.L. Nguyen, W. Stahl and J.T. Hougen, *J. Mol. Spectrosc.*, 2016, **318**, 91.
- [70] H.V.L. Nguyen and W. Stahl, *ChemPhysChem*, 2011, **12**, 1900.